

# Ti/C-3Ni/Al as a Replacement Time Delay Composition

Eric J. Miklaszewski,<sup>[a]</sup> Jay C. Poret,<sup>[b]</sup> Anthony P. Shaw,<sup>[b]</sup> Steven F. Son,<sup>[a]</sup> and Lori J. Groven<sup>†\*[a]</sup>

**Abstract:** Replacement reactive systems for the tungsten delay composition (W/BaCrO<sub>4</sub>/KClO<sub>4</sub>/diatomaceous earth) are needed due to recent concerns over the toxicity of hexavalent chromium and perchlorates. Systems based on condensed phase reactions, that are typically used in combustion synthesis (e.g., Ti/C or Ni/Al) are of interest as replacements due to their wide range of combustion velocities and potentially low environmental impact. In this work, the combustion characteristics of the Ti/C-3Ni/Al reactive system were examined in microchannels with inner diameters ranging from 3.0–6.0 mm (i.e., similar to that of a common delay housing). It was found that this reactive system could be tailored to overcome the heat losses associated with small diameter microchannels by changing the relative amounts of Ti/C and 3Ni/Al. At 40 wt.-% Ti/C con-

tent, the failure diameter was found to be between 3.0 and 4.0 mm, while at 30 wt.-% Ti/C the failure diameter was between 4.8 and 6.0 mm. Measured combustion temperatures in metal microchannels were approximately 1700 K while those of unconfined pellets were around 100 K greater. Increasing Ti/C content resulted in faster combustion velocities while decreasing microchannel diameter resulted in slower combustion velocities. At these small sizes the effects of adding a thermal barrier (specifically Grafoil™) to minimize radial heat losses to the microchannel were shown to be minimal with respect to combustion velocity. The Ti/C-3Ni/Al system was shown to be a suitable delay fuze composition with tunable combustion velocities ranging from 2.1–38.1 mm s<sup>-1</sup> in aluminum microchannels with diameters ranging from 4.0–6.0 mm.

**Keywords:** Delay fuze · Microchannels · Critical diameter · Stability · Combustion synthesis

## 1 Introduction

Many of today's pyrotechnic time delay compositions contain environmentally hazardous and toxic materials including heavy metals, chromates, and perchlorates (e.g., BaCrO<sub>4</sub>, PbCrO<sub>4</sub>, and KClO<sub>4</sub>). Even though these materials face increasing regulatory scrutiny [1–3], they are still in widespread use in military delay systems due to proven reliability and a wide range of combustion velocities [4]. The most versatile of these compositions, the W/BaCrO<sub>4</sub>/KClO<sub>4</sub>/diatomaceous earth composition [5], may be tuned to give combustion velocities ranging from 0.6–150 mm s<sup>-1</sup> [5,6]. This composition is also "gasless" (producing less than 10 mL g<sup>-1</sup> of gas) allowing it to be used in sealed housings. Several recent efforts describe metal/metal oxide compositions that are capable of propagating at relatively slow rates (less than 5 mm s<sup>-1</sup>), although they either contain environmentally questionable materials or produce excessive gas upon combustion [7–11]. Replacement compositions that are environmentally benign, gasless, and are capable of reproducible slow combustion velocities are needed to comply with environmental regulations while also providing an adequate degree of performance and versatility.

As potential replacements for traditional W/BaCrO<sub>4</sub>/KClO<sub>4</sub> compositions, condensed phase reactions (e.g., Ti/C or Ni/Al) are of particular interest because a wide range of combustion velocities (1–300 mm s<sup>-1</sup>) are achievable, depending on the constituents and stoichiometry [12,13]. An

additional benefit of such systems is their gasless nature. While such reactions have been widely investigated and used for the large scale production of ceramic and intermetallic materials, they have not been thoroughly studied in small channels (e.g., less than 6 mm diameter). At these small diameters heat losses are substantial, especially in metal channels, and may lead to combustion front instabilities (oscillations, pulsations) or extinction. This is a particular challenge if such reactive systems are to be used as military time delays, as the housings are often die-cast zinc alloy or aluminum with internal diameters as small as 5.0 mm [10].

Exothermic reactive systems with high heats of reaction, such as Ti/C ( $\Delta H_r = -3079 \text{ J g}^{-1}$ ) [14], Ti/B<sub>4</sub>C ( $\Delta H_r =$

[a] E. J. Miklaszewski, S. F. Son, L. J. Groven  
School of Mechanical Engineering  
Purdue University  
West Lafayette, IN, USA  
\*e-mail: lori.groven@sdsmt.edu

[b] J. C. Poret, A. P. Shaw  
Pyrotechnics Technology and Prototyping Division  
US Army RDECOM-ARDEC  
Picatinny Arsenal, NJ, USA

[†] Current Address:  
Chemical & Biological Engineering Department  
South Dakota School of Mines & Technology  
Rapid City, SD, USA

## Report Documentation Page

*Form Approved*  
*OMB No. 0704-0188*

Public reporting burden for the collection of information is estimated to average 1 hour per response, including the time for reviewing instructions, searching existing data sources, gathering and maintaining the data needed, and completing and reviewing the collection of information. Send comments regarding this burden estimate or any other aspect of this collection of information, including suggestions for reducing this burden, to Washington Headquarters Services, Directorate for Information Operations and Reports, 1215 Jefferson Davis Highway, Suite 1204, Arlington VA 22202-4302. Respondents should be aware that notwithstanding any other provision of law, no person shall be subject to a penalty for failing to comply with a collection of information if it does not display a currently valid OMB control number.

1. REPORT DATE <b>07 NOV 2013</b>	2. REPORT TYPE <b>N/A</b>	3. DATES COVERED <b>-</b>			
4. TITLE AND SUBTITLE <b>Ti/C-3Ni/Al as a Replacement Time Delay Composition</b>		5a. CONTRACT NUMBER			
		5b. GRANT NUMBER			
		5c. PROGRAM ELEMENT NUMBER			
6. AUTHOR(S) <b>Eric J. Miklaszewski, Jay C. Poret, Anthony P. Shaw, Steven F. Son, Lori J. Groven</b>		5d. PROJECT NUMBER			
		5e. TASK NUMBER			
		5f. WORK UNIT NUMBER			
7. PERFORMING ORGANIZATION NAME(S) AND ADDRESS(ES) <b>Pyrotechnics Technology and Prototyping Division US Army RDECOM-ARDEC, Picatinny Arsenal, NJ</b>		8. PERFORMING ORGANIZATION REPORT NUMBER			
		10. SPONSOR/MONITOR'S ACRONYM(S)			
9. SPONSORING/MONITORING AGENCY NAME(S) AND ADDRESS(ES)		11. SPONSOR/MONITOR'S REPORT NUMBER(S)			
		12. DISTRIBUTION/AVAILABILITY STATEMENT <b>Approved for public release, distribution unlimited</b>			
13. SUPPLEMENTARY NOTES <b>The original document contains color images.</b>					
14. ABSTRACT <b>The Ti/C-3Ni/Al system was shown to be a suitable delay fuze composition with tunable combustion velocities ranging from 2.138.1 mm/s in aluminum microchannels with diameters ranging from 4.06.0 mm.</b>					
15. SUBJECT TERMS					
16. SECURITY CLASSIFICATION OF:			17. LIMITATION OF ABSTRACT <b>SAR</b>	18. NUMBER OF PAGES <b>10</b>	19a. NAME OF RESPONSIBLE PERSON
a. REPORT <b>unclassified</b>	b. ABSTRACT <b>unclassified</b>	c. THIS PAGE <b>unclassified</b>			

$-3610 \text{ J g}^{-1}$ ) [15], Ti/2B ( $\Delta H_f = -5523 \text{ J g}^{-1}$ ) [14], may be ideal for overcoming the high heat losses inherent to sub-cm channels while maintaining moderate combustion velocities. In these cases, steady combustion may be possible due to a relatively low ratio of heat loss to heat generation in the reaction zone. For example, Pacheco et al. [16] studied Ti/2B and Ti/C with copper and aluminum diluents and showed that diameter had no effect on the combustion velocity until extinction was observed at diameters as small as 6.48 mm. In an unconfined pellet configuration, Roy and Biswas [17] studied Ti/2B and Ti/B and showed that diameters below 6.0 mm would quench. At smaller scales (sub-mm), Tappan et al. [18] conducted experiments using Ti/B<sub>4</sub>C with Ni/Al as a diluent/binder in borosilicate glass capillaries. A steady reaction was shown to propagate at diameters as small as 0.4 mm and decreasing capillary size did not significantly decrease combustion front velocity until the failure diameter was reached.

The objective of this work was to extend our preliminary efforts on two condensed phase reactions, Ti/C and 3Ni/Al, as potential time delay compositions [19]. Specifically, failure diameter and combustion wave velocity were investigated by varying the overall mixture exothermicity with combinations of the highly exothermic Ti/C reaction and the less exothermic 3Ni/Al reaction. The effect of system heat loss to heat generation was also explored by varying the consolidated density, the addition of a radial thermal barrier, and by changing the microchannel diameter (3.0–6.0 mm) and material (aluminum, stainless steel, quartz). Experimental combustion temperatures measured with micro-thermocouples are also presented and correlated to the measured combustion wave velocities.

## 2 Experimental Methods

### 2.1 Reactive Compositions

Nominal sizing and vendor information for the powders used in these experiments are summarized in Table 1. The mixtures were dry mixed using a Resodyn LabRAM mixer at 80% intensity in two minute intervals with a one minute wait time between intervals for a total of 6 min of mixing. The mixing order was observed to have a measurable effect on the combustion velocity of the composition. For example, if all constituents (Ti, C, Ni, Al) were mixed together

**Table 1.** Vendor information for reactant powders used.

Powder	Vendor	Reported Size
Al	AAE	1–5 $\mu\text{m}$
C (Lamp Black)	Spectrum Chemical	sub- $\mu\text{m}$
Diatomaceous Earth	Sigma Aldrich	15.4 $\mu\text{m}$
Fe <sub>2</sub> O <sub>3</sub> (III)	Firefox Enterprises	< 44 $\mu\text{m}$
Ni	Novamet	3–11 $\mu\text{m}$
Ti	Alfa Aesar	< 44 $\mu\text{m}$
Zr	Alfa Aesar	< 44 $\mu\text{m}$

er initially then only partial propagation was observed. Therefore, each reactive system (Ti/C, 3Ni/Al) was first mixed separately in stoichiometric proportion with Ti/C being 79.9wt.-% Ti and 20.1wt.-% C and 3Ni/Al being 86.7wt.-% Ni and 13.3wt.-% Al. The premixed Ti/C and 3Ni/Al were then mixed together using the same mixing procedure.

### 2.2 Combustion Experiments

Metal tubes with inner (outer) diameters of 3.0 mm (8.5 mm), 4.0 mm (8.9 mm), 4.8 mm (9.3 mm) and 6.0 mm (10.0 mm) were used for the experimental microchannels. A microchannel diameter matching that of a typical fielded delay housing (4.8 mm ID) was used as the baseline diameter in this study [8]. Channels were either made from 2024 grade T3 aluminum (Al) or 304L stainless steel (SS). Dimensions were selected so that the thermal mass (heat capacity) of the Al channels was the same for all diameters. The average mass of the aluminum channels (regardless of diameter) was  $2.126 \pm 0.005 \text{ g}$ . For some experiments, a 0.25 mm graphite foil (Grafoil™ supplied by Mineral Seal Corp.) liner was inserted into the channel. Also, a subset of experiments used quartz tubes with inner diameters of 4.9 and 6 mm (1.0 mm wall thickness). The length of all microchannels used was 15.2 mm. Reactive compositions were pressed to a stop using a Carver 12 t press so that desired consolidated densities ( $\pm 1\%$ ) were achieved. The igniter used in this study, referred to as A1A, is a common pyrotechnic composition composed of 65wt.-% Zr, 25wt.-% Fe<sub>2</sub>O<sub>3</sub> and 10wt.-% diatomaceous earth. Specifications can be found in Table 1. Approximately 1.0 mm of A1A was pressed on either end of the channel to a consolidated density of  $3.0 \text{ g cm}^{-3}$  both as an ignition increment and to optically signal when the reaction front reached the end of the microchannel. The various experimental configurations are shown in Figure 1. Due to the number of experimental configurations studied in this work only repeatability of selected experiments was evaluated. This included five ex-

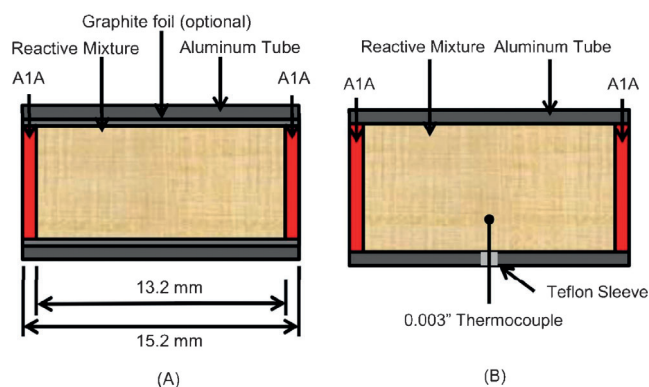


**Figure 1.** (A) Baseline microchannel configuration. (B) Microchannel with micro-thermocouple port for combustion temperature measurements.

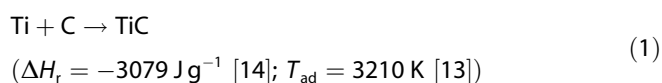
periments each of the baseline composition at consolidated densities of 40, 50 and 60% TMD, and a varied number of experiments for each configuration as noted in Table 4. Unless noted, one experiment was performed at other conditions assessed.

The A1A ignition increment was ignited with 30 gauge nichrome wire. A Sony Handycam digital video camera (30 fps) was used to record the experiment and the system combustion velocity was determined by dividing the length of the microchannel by the time between first light (A1A ignition) on either side of the channel. In some experiments, an unconfined pellet configuration (no microchannel) or a slitted (0.5 mm slit) microchannel was used to allow the combustion front to be observed. These experiments were imaged using a Vision Research Phantom v7.3 high speed camera at 1000 frames per second. The temperature profile of the reacting composition was measured in situ by inserting a 0.20 mm B-type Omega thermocouple through a micro-thermocouple port as shown in Figure 1B. To measure the external temperature of the microchannel, 0.25 mm K-type Omega thermocouples were used.

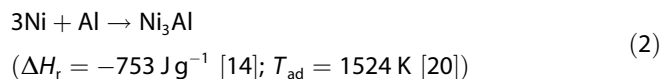
### 3 Results and Discussion

#### 3.1 Thermochemical Considerations

In this study two condensed phase reactions were considered:



and



Even at small diameters, the Ti/C reaction typically propagates too fast for most delay applications while the 3Ni/Al reactive system does not self-propagate at any diameter due to its low combustion temperature. According to the Merzhanov criterion if the predicted adiabatic combustion temperature is below 1800 K, the reaction may not be self-propagating [21].

Therefore, it was anticipated that the high heat losses introduced by the microchannel might be overcome by the highly exothermic Ti/C reaction and the combustion velocity could be tuned by the addition of 3Ni/Al, which essentially acts as a diluent. The 3Ni/Al system was selected because slower combustion wave velocities were achieved than when elemental nickel was used as the diluent. Given the high combustion velocity of Ti/C, thermochemical predictions (calculated using HSC v7.0 [22]) were used to target a composition with a moderate adiabatic combustion temperature by using the 3Ni/Al system as a diluent.

**Table 2.** Adiabatic combustion temperatures and predicted heats of formation for the combined Ti/C-3Ni/Al reactive system.

Composition #	Reactive Systems		$T_{\text{ad}}$ [K]	$\Delta H_f$ [J g <sup>-1</sup> ]
	Ti/C [wt.-%]	3Ni/Al [wt.-%]		
1	30	70	2163	-1451
2*	35	65	2257	-1567
3	40	60	2349	-1683

\*Baseline composition used in this work.

The calculated adiabatic temperatures and heats of formation are presented in Table 2. To effectively slow the combustion velocity, an adiabatic combustion temperature in the range of 2100 K to 2400 K was targeted. As shown in Table 2, compositions varying from 30–40wt.-% Ti/C fell within this range. Initial screening of these compositions resulted in the slowest combustion velocities without failure at the diameters of interest [19]. In reality, the adiabatic combustion temperatures will never be reached due to the very small scale of the experiments. The experimental combustion temperatures of these compositions were measured in situ and are presented later.

#### 3.2 Effect of Consolidated Density on Combustion Wave Velocity

It is well documented for condensed phase reactions that the combustion front velocity is strongly influenced by the consolidated density [20]. For example, Yeh [23] found that at a consolidated density of 55% of the theoretical maximum density (TMD) Ni/Al will propagate at a rate of 22 mm s<sup>-1</sup>, but at 65% TMD propagates at 48 mm s<sup>-1</sup>. For these reactions quenching or failure occurs when the density of the compact is either too low or high. At low densities, the reacting compact may not transfer enough energy to react subsequent layers, while at high densities the increased thermal conductivity of the compact may conduct heat away from the reaction zone too quickly resulting in self-quenching of the reaction. Initial screening of the Ti/C-3Ni/Al system in 4.8 mm Al microchannels found that the reaction was self-sustaining only at compositions containing in excess of 35wt.-% Ti/C [19]. This result is specific to the powders used in this study since the overall reactivity is dependent on the particle size, morphology, and intimacy of the reactants. Therefore, 35wt.-% Ti/C (composition #2) was selected as the baseline. The effect of consolidated density on the combustion velocity for 4.8 mm and 6.0 mm Al microchannels is shown in Figure 2. Consolidated densities were limited to ≥ 40% TMD due to difficulties retaining compact integrity at lower values. For a diameter of 4.8 mm full propagation was observed at consolidated densities ranging from 40–56% TMD and the combustion velocity increased from 2.06 mm s<sup>-1</sup> (40% TMD) to 3.4 mm s<sup>-1</sup> (56% TMD). Repeatability was assessed with five experiments at consolidated densities of 40, 50 and 60% TMD

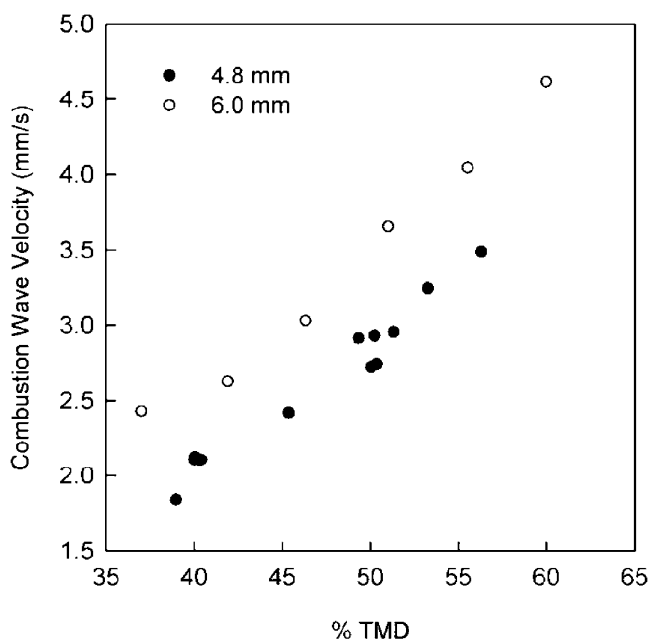


**Figure 2.** Combustion wave velocity of Ti/C-3Ni/Al(35/65wt.-%) as a function of packing density in 4.8 and 6.0 mm inner diameter Al microchannels.

and was found to be consistent. At 40 and 50% TMD the combustion velocity was measured to be  $2.06 \pm 0.12$  and  $2.85 \pm 0.11$   $\text{mm s}^{-1}$  respectively. While at 60% TMD the reaction propagated  $4.02 \pm 0.55$  mm down the length of the channel and then quenched in all cases. Increasing the microchannel diameter from 4.8 to 6.0 mm increased the

range of densities where full propagation resulted (up to 60% TMD) as well as the observed combustion velocities. At a consolidated density of 55% TMD, the reaction propagates approx.  $0.55$   $\text{mm s}^{-1}$  faster in a 6.0 mm diameter microchannel than in the 4.8 mm channel due to a larger ratio of heat generation to heat loss (recall both microchannels have the same thermal mass). At smaller diameters (3.0 and 4.0 mm) the reaction propagated 2.0 to 4.0 mm down the channel and then quenched. Therefore, the failure diameter for composition #2 was found to be between 4.0 and 4.8 mm.

### 3.3 Effect of Minimizing Radial Heat Loss with Thermal Barriers

Failure diameter and combustion velocity can also be influenced by minimizing the radial heat losses to the microchannel. Implementation of a low thermal conductivity (approx.  $5$   $\text{W m}^{-1} \text{K}^{-1}$  radially [24]) 0.25 mm thermal barrier (Grafoil™) is illustrated in Figure 1A. Previously, such a barrier was shown to have several beneficial effects on the overall stability and combustion front velocity for the Ti/C-Ni/Al- $\text{Al}_2\text{O}_3$  system [19]. It should be noted that when introducing the barrier, the inner diameter of the microchannel is effectively reduced (i.e., 6.0 mm becomes 5.5 mm) and the quantity of the reactive composition is also reduced. Interestingly, at a consolidated density of 50% TMD in a 6.0 mm Al microchannel adding the Grafoil™ barrier resulted in a negligible difference in combustion velocity (Figure 3A) for reactive composition #2. For the 4.8 mm channel lined with Grafoil™ (4.3 mm inner diameter) a noticeably smaller range of consolidated densities at which the reaction fully

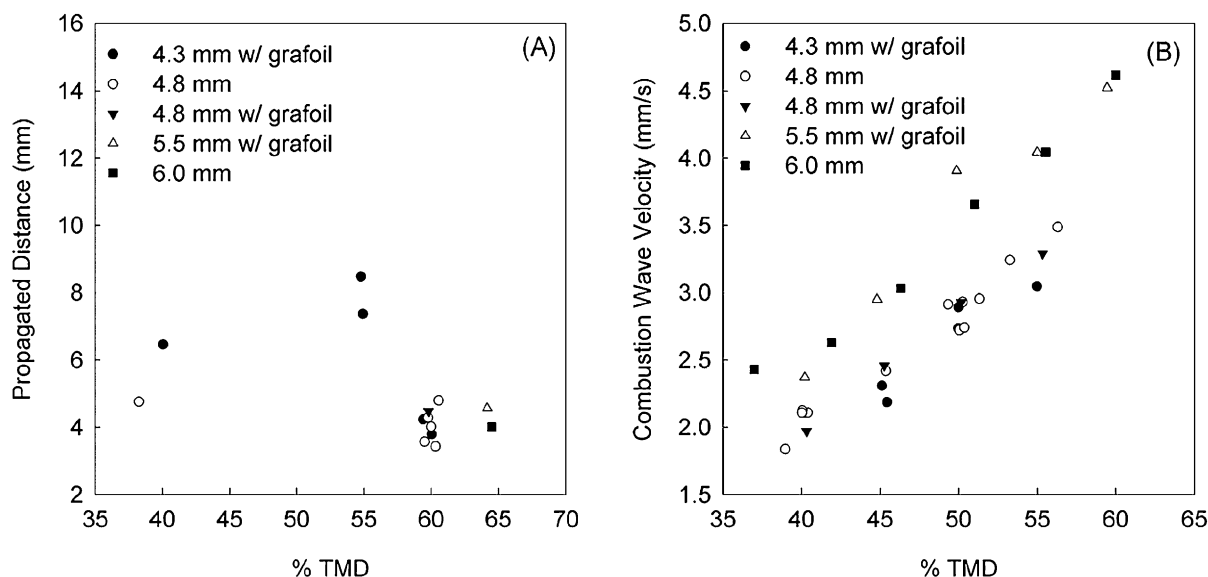


**Figure 3.** (A) Propagated distance and (B) combustion wave velocity for Ti/C-3Ni/Al(35/65wt.-%) with and without Grafoil™. Note that for propagated distance only partial propagations are plotted for clarity. Full propagation distance is 13.2 mm. Effective inner diameter is reported.

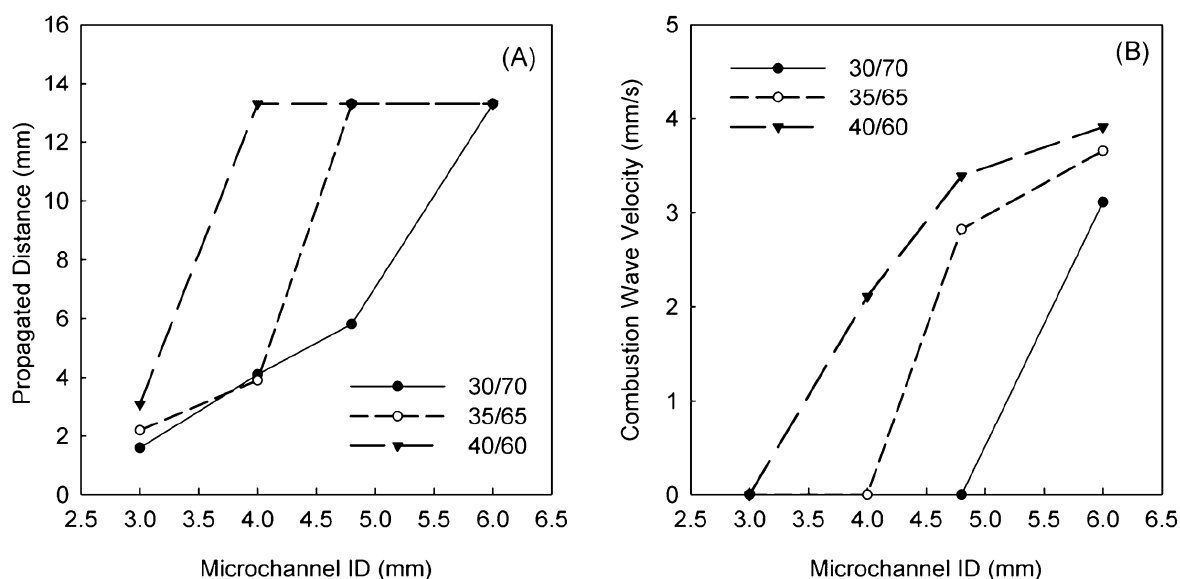


**Figure 4.** (A) Propagated distance and (B) combustion wave velocity as a function of Ti/C-3Ni/Al composition ratio at 50% TMD.

propagated (45 to 50% TMD) was observed. Furthermore, two of three experiments conducted at 55% TMD did not fully propagate, which indicated that the failure diameter was being approached. Additionally, direct comparison of microchannels with an effective inner diameter of 4.8 mm (with and without Grafoil™) also resulted in little difference being observed in the combustion velocity (Figure 3B). This is in contrast to our previous results for the Ti/C-Ni/Al-Al<sub>2</sub>O<sub>3</sub> system where the overall propagation rate increased along with the range of consolidated densities where full propagation was observed [19]. Therefore, for these compositions the added benefits of reducing the radial heat loss with Grafoil™ was not significant enough to observe a change in combustion velocity.

### 3.4 Tailoring Combustion Wave Velocity through Exothermicity

An important feature of the tungsten delay composition is its wide range of combustion velocities enabling multiple application requirements to be met. Therefore, it is highly desired to have replacement compositions that can also be tuned to propagate at various diameters, and at selected velocities for a given application. To evaluate the versatility of the Ti/C-3Ni/Al reactive system the reaction exothermicity was modified by changing the Ti/C content (30–40 wt.-%). Figure 4 presents a series of experiments conducted at a consolidated density of 50% TMD, presented as a function of microchannel diameter. As previously discussed, the baseline composition (35 wt.-% Ti/C) ceased to fully propagate at microchannel diameters between 4.0 and 4.8 mm. By increasing the Ti/C content by 5 wt.-% (composition #3), the reaction was exothermic enough to fully propagate at a channel diameter of 4.0 mm whereas the baseline com-

position was not. Furthermore, decreasing the Ti/C content by 5 wt.-% to 30 wt.-% (composition #1) reduces the exothermicity so that the reactive composition only fully propagated at the largest diameter (i.e., 6.0 mm) as shown in Figure 4a. The combustion velocity of the reactive system Ti/C-3Ni/Al, where relative Ti/C content is less than 40 wt.-%, has tunable combustion velocities as low as 2.1 mm s<sup>-1</sup> (3.0 mm ID) as shown in Figure 4B. It should be noted that a maximum combustion velocity of 38.1 mm s<sup>-1</sup> was observed for experiments conducted with 100 wt.-% Ti/C in a 6.0 mm aluminum microchannel. This result closely matches previous reports that found the Ti/C composition to have a combustion velocity of 32.8 mm s<sup>-1</sup> in an unconfined pellet configuration [21]. These results illustrate that reactions such as Ti/C-3Ni/Al can be tailored to overcome the high heat loss conditions typical of metal microchannels that would typically lead to quenching and failure.

### 3.5 Effect of Microchannel Material

It is well documented that the delay housing material can have a significant effect on the combustion velocity of delay compositions [4, 7]. Highly conductive materials such as aluminum will transfer thermal energy along the length of the tube effectively preheating the composition and increase the resulting combustion velocity [4]. However, for reactive systems such as Ti/C-3Ni/Al the effect of different housing materials (microchannels) on the combustion behavior has not previously been documented. To verify that thermal energy is being transferred more quickly for the Al vs. the SS microchannels the thermal profile of the channel was measured with a thermocouple placed 12.7 mm from the ignition increment. For these experiments, only the standard A1A ignition increment and a non-reacting

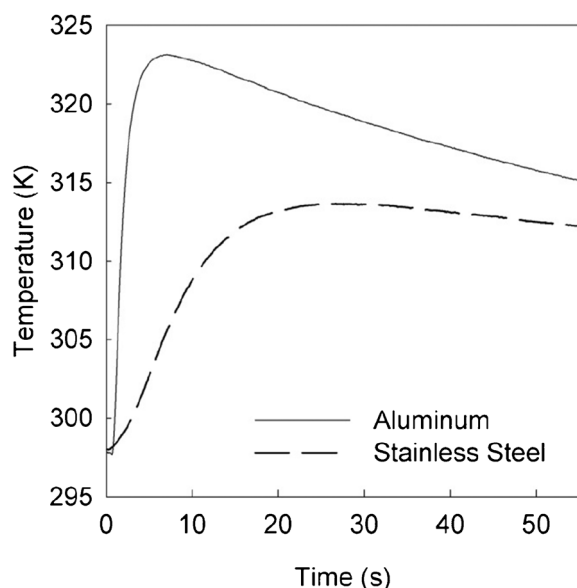


**Figure 5.** Temperature profiles from ignition contribution experiments. A1A ignition increment and nickel powder at 50% TMD in Al and SS microchannels.

powder (50% TMD Ni powder) were pressed into the microchannel. As shown in Figure 5, a peak temperature was reached in 6.4 seconds for the Al microchannel while it took 28.3 seconds for the peak temperature to be reached for the SS channel. From these experiments, it is clear that the more conductive material, Al, transfers thermal energy down the channel much more quickly and will effectively preheat the reactants [26].

In order to observe the affect this will have on the combustion behavior of the Ti/C-3Ni/Al reactive system experiments were performed in 4.8 mm Al and SS microchannels, 4.9 mm quartz microchannels (1 mm wall thickness), and a special thin wall SS microchannel (denoted as SS\*\*). The baseline composition (35 wt.-% Ti/C) at a consolidated density of 55% TMD was considered. The thermal properties of the microchannels as well as observed combustion velocities are detailed in Table 3.

It is expected that some effect of preheating might be observed when comparing the 4.8 mm Al and the SS mi-

crochannel. This was indeed the case as the reaction quenched after 6.7 mm when conducted in the SS microchannel but propagated at a combustion velocity of  $3.49 \text{ mm s}^{-1}$  in the Al microchannel. When the reaction was conducted in the quartz microchannel (even lower thermal conductivity) a similar combustion velocity to that observed for the Al microchannel was observed ( $3.42 \text{ vs. } 3.49 \text{ mm s}^{-1}$ ). This was interesting considering that without preheating effects a much slower combustion velocity or quenching was expected. To observe *only* a difference in thermal conductivity, microchannels with the same thermal mass (Al and thin wall SS\*\*) were used. In this case the effect of preheating was clear; for the thin wall SS\* microchannel the combustion velocity was only  $2.77 \text{ mm s}^{-1}$  vs. the  $3.49 \text{ mm s}^{-1}$  for the aluminum microchannel. Interestingly, the effect of preheating due to the microchannel was also observed for experiments conducted without microchannel confinement. The combustion velocity for an unconfined 4.8 mm pellet was even slower than when conducted in the thin walled SS\* microchannel ( $2.53 \text{ mm s}^{-1}$  vs.  $2.77 \text{ mm s}^{-1}$ ) even though the microchannel results in significantly higher heat losses. Similarly, for an unconfined 6.0 mm pellet the combustion velocity was slower than when the reaction was conducted in a 6.0 mm aluminum microchannel ( $3.61 \text{ mm s}^{-1}$  vs.  $4.04 \text{ mm s}^{-1}$ ). Therefore, when studying condensed phase reactives it is clear that microchannel choice will significantly affect the reaction propagation and in order to develop a robust replacement composition, the delay housing material and mass remains a critical consideration.

### 3.6 Combustion Stability

For condensed phase reactives, combustion stability is highly dependent on combustion temperature, activation energy and heat release [25]. Therefore, it is expected that by introducing significant heat losses from the microchannel that the reaction might be driven towards combustion instabilities (pulsations, oscillations, or quenching). While combustion velocities for the combined system (Ti/C-3Ni/Al) were consistent in confined microchannel experiments, a stable combustion mode must be verified for development of a robust delay composition.

**Table 3.** Material properties of the microchannels [26] and combustion velocities for experiments with the baseline composition (35 wt.-% Ti/C) at a consolidated density of 50% TMD.

Microchannel Type	$\rho$ [ $\text{kg m}^{-3}$ ]	$\kappa$ [ $\text{W m}^{-1} \text{K}^{-1}$ ]	$mc_p$ [ $\text{J K}^{-1}$ ]	Combustion velocity [ $\text{mm s}^{-1}$ ]
4.8 mm Al	2780	151	1.9	3.49
6.0 mm Al	2780	151	1.9	4.04
4.8 mm SS	8027	16	3.1	Quenched (6.69 mm)
4.8 mm SS**	8027	16	1.7	2.77
4.9 mm Quartz	2230	1.4	0.5	3.42
4.8 mm pellet	–	–	–	2.53
6.0 mm pellet	–	–	–	3.61

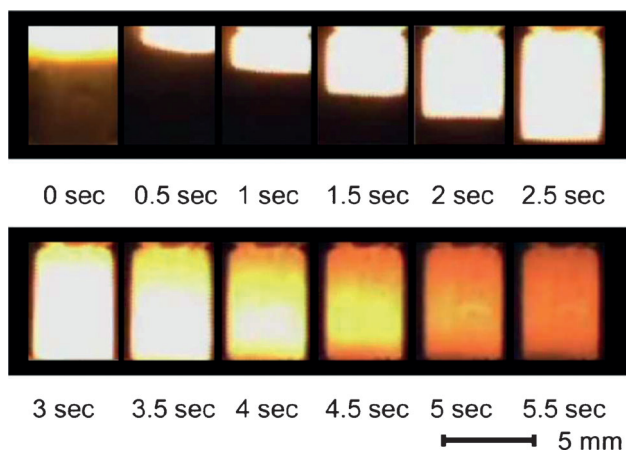


**Figure 6.** Images of the combustion front in a typical 4.8 mm diameter unconfined pellet experiment. (Composition #3 at 55% TMD).

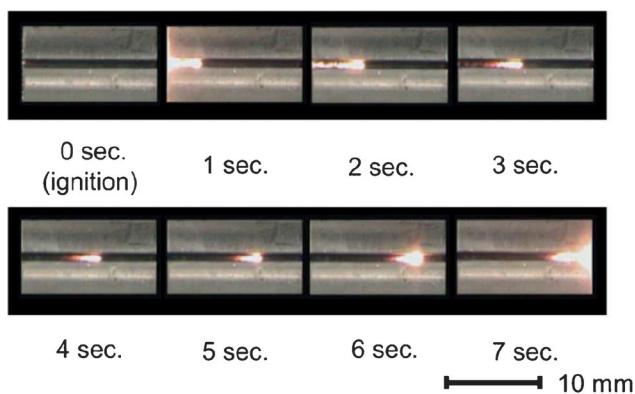


**Figure 7.** Images of the combustion front in a typical slit experiment. 4.8 mm aluminum microchannel with composition #2 at 50% TMD.

In stable layer by layer combustion, the reaction proceeds by first forming a melt layer of the lower melting point reactants. The remaining reactants then diffuse into this melt layer and exothermically react forming the next melt layer by which the reaction proceeds. While layer by layer combustion is common in condensed phase reactives, small oscillations can still result in a steady combustion velocity. Large oscillations however are observed to have sinusoidal type behavior with significant fluctuations in the combustion front position vs. time profile; this is often accompanied by low repeatability and generally leads to extinction [25].

To evaluate stability without heat losses to the microchannel, unconfined 4.8 mm diameter pellets were considered first. It should be noted that the unconfined pellets were shorter than the full length of the microchannels due to difficulties preparing relatively low density (55% TMD) pellets with an aspect ratio of over three. As shown in Figure 6, the combustion front appears to be steady and planar with no observable pulsations or oscillations. Due to the microchannel configuration, direct observation of the combustion wave front is not possible. Therefore, stability was observed by using slitted aluminum microchannels. A typical experiment is shown in Figure 7. While there are some differences between the fully confined channels and the slitted microchannels, these experiments allow some evaluation of the stability of the Ti/C-3Ni/Al system at these small sizes.

The stability was further assessed from the combustion front position vs. time ( $x-t$ ) plots as shown in Figure 8. For these experiments the measured velocities (Table 4) differ slightly from the reported system combustion wave velocities as the ignition increment is not included. For unconfined pellets stable combustion was observed for both

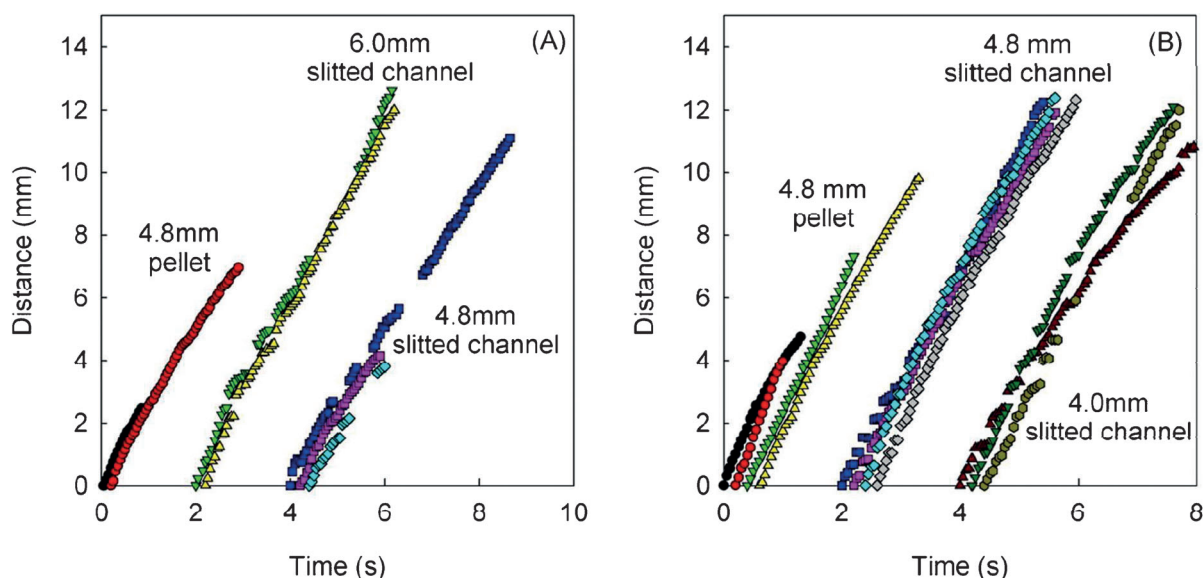


**Figure 8.** A) Combustion front position vs. time plots for Ti/C-3Ni/Al(35/65) at 55%TMD. B) Combustion front position vs. time plots for Ti/C-3Ni/Al(40/60) at 55% TMD. The x-intercept of this data is staggered for presentation clarity.



**Table 4.** Effect of microchannel diameter/type on combustion stability of Ti/C-3Ni/Al (35/65 wt.-%) at 55% TMD. FP/PP is the number of fully propagated experiments to partially propagated experiments.

Ti/C-3Ni/Al (35/65)				
Test Case	FP/PP	Prop. Dist. [mm]	Combustion Wave Velocity [mm s <sup>-1</sup> ]	( <i>x</i> vs. <i>t</i> ) <sub>slope</sub> [mm s <sup>-1</sup> ]
4.8 mm Al channel	2/0	–	3.62 ± 0.18	–
4.8 mm slitted Al channel	1/4	–	3.1	2.28
		6.06 ± 0.21*	–*	2.41 ± 0.06*
4.8 mm pellet	2/0	–	–	2.79 ± 0.40
6.0 mm Al Channel	1/0	–	4.04	–
6.0 mm slitted Al channel	2/0	–	3.62 ± 0.05	2.87 ± 0.01
Ti/C-3Ni/Al (40/60)				
Test Case	FP/PP	Prop. Dist. [mm]	Combustion Wave Velocity [mm s <sup>-1</sup> ]	( <i>x</i> vs. <i>t</i> ) <sub>slope</sub> [mm s <sup>-1</sup> ]
4.0 mm Al Channel	3/0	–	4.27 ± 0.07	–
4.0 mm slitted Al channel	3/0	–	4.31 ± 0.06	3.31 ± 0.50
4.8 mm Al channel	4/0	–	4.30 ± 0.17	–
4.8 mm slitted Al channel	4/0	–	4.29 ± 0.05	3.62 ± 0.14
4.8 mm pellet	4/0	–	–	3.87 ± 0.32

\*Signifies experiments that resulted in quenching.

compositions (35 and 40 wt.-% Ti/C) as indicated by the linear *x-t* profiles shown in Figure 8A, B. In the case of the microchannels introduction of the 0.5 mm slit resulted in the reaction being retarded as detailed in Table 4. For the baseline composition the combustion velocity was reduced by 0.51 and 0.42 mm s<sup>-1</sup> in the 4.8 and 6.0 mm Al channels respectively. This is due in part to reduced heat transfer to

the channel (approx. 5% reduction in microchannel mass). The combustion front analysis of the baseline composition (35 wt.-% Ti/C) in the larger 6.0 mm Al-slitted microchannel case showed steady combustion with a slope of 2.87 mm s<sup>-1</sup> (Figure 8A). However, when decreasing the diameter to 4.8 mm (approaching failure conditions for this composition), only one out of five of these experiments resulted in full propagation (Table 4). Importantly, both the fully propagating case and the cases where quenching occurred resulted in *x-t* profiles with essentially the same slope (velocity) as shown in Figure 8A. This clearly shows that even when combustion is on the verge of failure, a steady combustion front is observed up until the reaction can no longer provide enough heat to initiate the next layer of unreacted material.

The combustion front analysis of composition #3 (40 wt.-% Ti/C) in the 4.8 mm Al-slitted microchannel also shows a linear *x-t* profile with a slope of 3.62 mm s<sup>-1</sup> (Figure 8B). When decreasing the diameter to 4.0 mm (approaching failure conditions), the observed slope (velocity) decreases slightly to 3.31 mm s<sup>-1</sup> but is clearly steady and repeatable. Overall, based on the high repeatability of the fully confined microchannel experiments and the lack of observed combustion front oscillations, stable layer by layer type combustion is the dominant mode present for these combined reactive systems under these heat loss conditions.

### 3.7 Combustion Temperature Analysis

As shown in Figure 9, it is clear that the peak combustion temperature of the Ti/C-3Ni/Al reactive system is not significantly affected by radial heat losses to the microchannel. Between the 6.0 mm and 4.8 mm diameter microchannels,

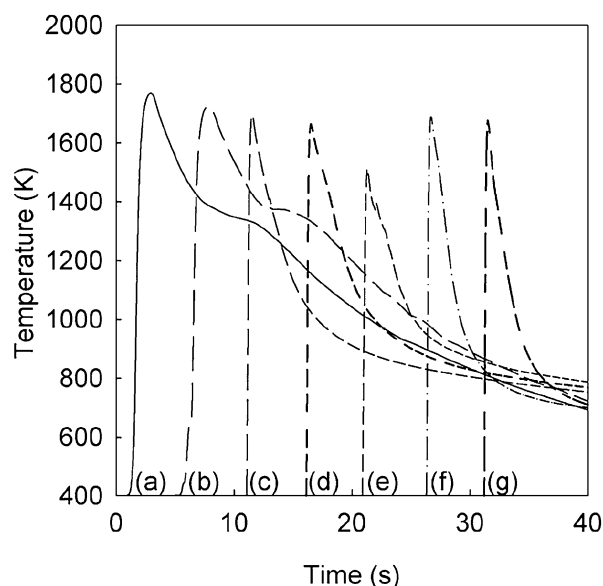


**Figure 9.** Ti/C-3Ni/Al combustion temperature profiles at various ratios in Al microchannels at 55% TMD. (a) (40/60), 6.0 mm pellet. (b) (35/65), 6.0 mm pellet. (c) (40/60), 6.0 mm Al channel. (d) (35/65), 6.0 mm Al channel. (e) (30/70), 6.0 mm Al channel. (f) (40/60), 4.8 mm Al channel. (g) (35/65), 4.8 mm Al channel.

**Table 5.** Combustion temperature predictions and measured peak combustion temperatures.

Combustion Temperatures				
Ti/C [wt.-%]	$T_{ad}$ [K]	4.8 mm channel, $T_c$ [K]	6.0 mm channel, $T_c$ [K]	6.0 mm pellet, $T_c$ [K]
30	2163.1	–	1511.7	–
35	2256.6	1676.3	1664.6	1719.3
40	2349.3	1688.3	1696.6	1769.7

**Table 6.** Characteristic cooling time for Ti/C-3Ni/Al reactive system in various configurations. The characteristic cooling time is defined as the time elapsed from the peak temperature to 800 K.

Ti/C [wt.-%]	4.8 mm channel, $\tau$ [s]	6.0 mm channel, $\tau$ [s]	6.0 mm pellet, $\tau$ [s]
30	–	16.4	–
35	4.6	17.4	27.0
40	5.2	19.2	29.8

less than 100 K decrease in combustion temperature was measured (Table 5). Additionally, changing the overall exothermicity resulted in only minor changes to the observed peak combustion temperature. However, rapid cooling is observed when the reaction is performed in the microchannel configuration. This is best represented by a characteristic cooling time - the time from the peak combustion temperature to 800 K. For example, the most exothermic composition (#3–40 wt.-% Ti/C) cools to 800 K in 19.2 s when performed in the 6.0 mm microchannel vs. 29.8 s when performed in an unconfined pellet configuration (Table 6). The characteristic cooling time for this composition is only 5.2 s when performed in the 4.8 mm microchannel. This illustrates the manner in which the critical diameter is realized for this system; heat is transferred from the reaction to the microchannel resulting in rapid cooling and hence the reaction can no longer ignite the next layer of material and quenches. Therefore, it is clear that system heat losses play a dominant role in determination of the combustion wave velocity and must be considered in the development of a robust delay element.

## 4 Conclusion

In this work, the combustion characteristics of the combined reactive system Ti/C-3Ni/Al were examined in small diameter metal tubes (3.0–6.0 mm ID). It was demonstrated that by varying the Ti/C content, the system can be tuned to propagate at various diameters resulting in a range of combustion wave velocities. For the range of Ti/C content studied (30–40 wt.-%), the failure diameter was shown to vary based on Ti/C content. At 40 wt.-% Ti/C, the failure diameter was between 3.0 and 4.0 mm while at 30 wt.-% Ti/C, the failure diameter was between 4.8 and 6.0 mm. For this system, it is clear that heat losses to the microchannel directly affect the observed combustion wave velocity. At

these small sizes, and for this system, the effects of adding a thermal barrier (i.e., Grafoil™) to minimize radial heat losses to the microchannel were shown to be minimal with respect to combustion velocity. Even with the high heat losses from metal microchannels, these compositions exhibited steady layer by layer combustion and also produced repeatable delay times over a wide range of consolidated densities. Overall, the Ti/C-3Ni/Al system has tunable range of combustion velocities ranging from 2.1–38.1 mm s<sup>-1</sup> in common delay diameters and could be considered as a potentially less toxic replacement for the W/BaCrO<sub>4</sub>/KClO<sub>4</sub>/diatomaceous earth formulation.

## Acknowledgments

This work was supported at Purdue University by the US Army RDECOM Environmental Quality Technology Program via the Armament Research, Development and Engineering Center under Contract #W15QKN-09-C-0121. The authors would like to thank Prof. Timothee Pourpoint for the use of his MATLAB code for the analysis of high speed images.

## References

- [1] K. Sellers, W. Alsop, S. Clough, M. Hoyt, B. Pugh, K. Weeks, *Perchlorate: Environmental Problems And Solutions*, CRC Press Taylor & Francis Group, Boca Raton, FL, USA, 2007.
- [2] J. Guertin, J. A. Jacobs, C. P. Avakian, *Chromium (VI) Handbook*, CRC Press, Boca Raton, FL, USA, 2004. p. 491–564.
- [3] *Toxicological Profile for Barium and Barium Compounds*, U.S. Agency for Toxic Substances and Disease Registry, Washington, DC, USA, 2007.
- [4] M. A. Wilson, R. J. Hancox, *Pyrotechnic Chemistry: Pyrotechnic Reference Series No. 4*, Journal of Pyrotechnics, Inc., Whitewater, CO, USA, 2004.
- [5] *Tungsten Delay Composition*, Military Specification MIL-T-23132A, 1972.

- [6] E. Shachar, A. Gany, Investigation of Slow-Propagation Tungsten Delay Mixtures, *Propellants Explos. Pyrotech.* **1997**, *22*, 207–211.
- [7] L. Kalombo, O. Del Fabbro, C. Conradie, W. W. Focke,  $Sb_6O_{13}$  and  $Bi_2O_3$  as Oxidants for Si in Pyrotechnic Time Delay Compositions, *Propellants Explos. Pyrotech.* **2007**, *32*, 454–460.
- [8] D. Swanepoel, O. Del Fabbro, W. W. Focke, C. Conradie, Manganese as Fuel in Slow-Burning Pyrotechnic Time Delay Compositions, *Propellants Explos. Pyrotech.* **2010**, *35*, 105–113.
- [9] J. C. Poret, A. P. Shaw, L. J. Groven, G. Chen, K. D. Oyler, Environmentally Benign Pyrotechnic Delays, *38th International Pyrotechnics Seminar*, Denver, CO, USA, June 10–15, **2012**.
- [10] J. C. Poret, A. P. Shaw, C. M. Csernica, K. D. Oyler, D. P. Estes, Development and Performance of the W/ $Sb_2O_3$ / $KIO_4$ /Lubricant Pyrotechnic Delay in the US Army Hand-Held Signal, *Propellants Explos. Pyrotech.* **2012**, *38*, published online.
- [11] J. C. Poret, A. P. Shaw, C. M. Csernica, K. D. Oyler, J. A. Vanatta, G. Chen, Versatile Boron Carbide-Based Energetic Time Delay Compositions, *ACS Sus. Chem. Eng.* **2013**, published online.
- [12] S. D. Dunmead, Z. A. Munir, J. B. Holt, Temperature Profile Analysis in Combustion Synthesis: II, Experimental Observations, *J. Am. Ceram. Soc.* **1992**, *75*, 180–188.
- [13] A. Varma, J.-P. Lebrat, Combustion Synthesis of Advanced Materials, *Chem. Eng. Sci.* **1992**, *47*, 2179–2194.
- [14] S. H. Fischer, M. C. Grubelich, A Survey of Combustible Metals, Thermites, and Intermetallics for Pyrotechnic Applications, *32nd AIAA/ASME/SAE/ASEE Joint Propulsion Conference*, Lake Buena Vista, FL, USA, July 1–3, **1996**.
- [15] P. Mogilevsky, E. Y. Gutmanas, I. Gotman, R. Telle, Reactive Formation of Coatings at Boron Carbide Interface with Ti and Cr Powders, *J. Eur. Ceram. Soc.* **1995**, *15*, 527–535.
- [16] M. M. Pacheco, R. H. B. Bouma, L. Katgerman, Combustion Synthesis of  $TiB_2$ -Based Cermets: Modeling and Experimental Results, *Appl. Phys. A: Mater. Sci. Process.* **2007**, *90*, 159–163.
- [17] S. K. Roy, A. Biswas, Combustion Synthesis of  $TiB$  and  $TiB_2$  under Vacuum *J. Mater. Sci. Lett.* **1994**, *13*, 371–373.
- [18] A. Tappan, L. Groven, J. Miller, J. Puszynski, Combustion Synthesis in Gasless Pyrotechnics at Millimeter Geometries, *34th International Pyrotechnics Seminar*, Beaune, France, Oct. 8–11, **2007**.
- [19] E. J. Miklaszewski, S. F. Son, L. J. Groven, J. C. Poret, A. P. Shaw, G. Chen, Combustion Characteristics of Condensed Phase Reactions in Sub-Centimeter Geometries, *38th International Pyrotechnics Seminar*, Denver, CO, USA, June 10–15, **2012**.
- [20] A. Shiryaev, Thermodynamics of SHS Processes: An Advanced Approach, *Int. J. Self-Propag. High-Temp. Synth.* **1995**, *4*, 351–362.
- [21] J. J. Moore, H. J. Feng, Combustion Synthesis of Advanced Materials: Part I. Reaction Parameters, *Prog. Mater. Sci.* **1995**, *39*, 243–273.
- [22] A. Roine, *HSC Chemistry 7.0 User's Guide*, Report, Outotec Research Oy, **2009**.
- [23] C. L. Yeh, Effects of TiC addition on combustion synthesis of NiAl in SHS mode, *J. Alloys Compd.* **2005**, *398*, 85–93.
- [24] *Typical Grafoil Sheet Properties*, Report, Professional Plastics, **2013**.
- [25] K. G. Shkadinskii, B. I. Khaikin, A. G. Merzhanov, Propagation of a Pulsating Exothermic Reaction Front in the Condensed Phase, *Fiz. Goreniya Vzryva.* **1971**, *1*, 19–28.
- [26] F. Cardarelli, *Materials Handbook*, 2 ed, Springer-Verlag, London **2008**.

Received: August 6, 2013  
Revised: September 11, 2013  
Published online: November 7, 2013